

Calculation of the near field of aggregates of arbitrary spheres

Hongxing Xu

Division of Solid State Physics, Lund University, Box 118, S-22100, Sweden

Received August 4, 2003; revised manuscript received December 10, 2003; accepted December 11, 2003

We study a numerical method of calculating the near field of ensembles of arbitrary spheres by extending Mie theory. A recursive method based on the orders of scattering is presented. This method represents a concise way to calculate the near field of aggregates of any number of arbitrary spheres. Numerical examples are given to show its validity. © 2004 Optical Society of America

OCIS codes: 240.6680, 290.4020.

1. INTRODUCTION

Recently, there has been significant focus on near-field optics,¹ mainly as a result of rapid development in the following fields: (1) high spatial resolution of scanning near-field optical microscopy,^{1–3} (2) single-molecule spectroscopy by surface-enhanced Raman scattering,^{4–6} (3) nanodevices based on surface-plasmon photonic forces,^{7,8} and (4) quantum-optical processes in photonic crystals.⁹ In these fields, the calculation of the near field of ensembles of nanoparticles is a fundamental theoretical issue. However, as is well known, the tedious calculation processes for those multiple scatterers challenge both the numerical methods and computational capacities.^{1,10}

When the nanoparticles can be simplified to spheres, the analytical solution to the light scattering can be obtained by extending Mie theory.¹¹ Basically, there are two kinds of treatment. The first one is to consider the boundary conditions of all the particles at once to obtain a super-matrix, the so called T-matrix.^{12–14} In principle, the light scattering of aggregates can then be solved. It is true that the T-matrix treatment is successful for far-field calculations, e.g., for extinction–scattering–absorption spectra.^{13,14} However, for calculations of near field, this method would not really be successful for aggregates composed of more than two particles. The reason is mainly that the entangled interparticle couplings among many particles will increase the size of the scattering matrix tremendously, and thus, expedient calculations become difficult. The second treatment is based on orders of scattering, which consist of a sum of simple scattering events from single particles in which the boundary conditions are considered separately in each scattering event. Therefore, the full-boundary-condition problem is turned into a problem of multiple scattering with some translation rules between the scatterers. For the ensemble of two particles, the solution was given by Fuller.¹⁵ Recently, we have found a simple way to sort out the order of scattering thoroughly for ensembles of any number of spheres.¹⁶ Although the right order of scattering events is necessary for the correct calculations, the tedious calculation process is still the obstacle for large aggregates.

In the paper a recursive method is presented that is

based on the method of orders of scattering for aggregates composed of any number of spheres. The method starts with two particles and then uses recursion to obtain the solution for any number of particles. This paper is organized as follows. In Section 2 we start with the extended Mie theory. In Section 3 we show a recursive solution to sum single-scattering events for ensembles and to obtain the matrix representations that are suitable for calculations. In Section 4 two numerical examples are presented. In Section 5 a summary is given.

2. THEORY

On the basis of Mie theory,¹¹ both the incident electric field and the scattered electric field of the ensemble of L spheres can be expanded in the form of the vector spherical harmonics as

$$\begin{aligned}
 {}^i\mathbf{E}_l &= \sum_{n=1}^{\infty} \sum_{m=-n}^n \sum_{p=1}^2 {}^iC_{mnp}^l |mn1p\rangle, \\
 {}^s\mathbf{E} &= \sum_{l=1}^{\oplus L} {}^s\mathbf{E}_l = \sum_{l=1}^{\oplus L} \sum_{n=1}^{\infty} \sum_{m=-n}^n \sum_{p=1}^2 {}^sC_{mnp}^l |mn3p\rangle,
 \end{aligned} \tag{1}$$

where ${}^iC_{mnp}^l$ and ${}^sC_{mnp}^l$ are the expansion coefficients for the vector spherical harmonics $|mnjp\rangle$ centered at the l th sphere, with $p = 1$ for \mathbf{M}_{mn}^j and with $p = 2$ for \mathbf{N}_{mn}^j , and $j = 1, 2, 3, 4$ corresponds to spherical functions j_n , y_n , $h_n^{(1)}$, $h_n^{(2)}$, respectively.¹⁷ The symbol \oplus means that the sum should occur in Cartesian coordinates. By summation of single-scattering events, the scattering coefficients ${}^sC_{mnp}^l$ are functions of the incident coefficients ${}^iC_{mnp}^l$, the corresponding Lorenz–Mie coefficients a_n^l and b_n^l , and the translation coefficients ${}^{lh}A_{mn}^{\mu\nu}$ and ${}^{lh}B_{mn}^{\mu\nu}$ between sphere l and sphere h ^{18,19} and are written as

$${}^sC_{mnp}^l = {}^L T_l({}^iC_{\mu\nu q}^h, a_v^h, b_v^h, {}^{lh}A_{mn}^{\mu\nu}, {}^{lh}B_{mn}^{\mu\nu}). \tag{2}$$

The corresponding magnetic fields are expanded as

$$\mathbf{H}_l^l = \frac{k}{i\omega\mu} \sum_{n=1}^{\infty} \sum_{m=-n}^n \sum_{p=1 \neq p'}^2 iC_{mnp}^l |mnlp\rangle,$$

$$\mathbf{H}_s = \frac{k}{i\omega\mu} \sum_{l=1}^{\oplus L} \mathbf{H}_s^l$$

$$= \frac{k}{i\omega\mu} \sum_{l=1}^{\oplus L} \sum_{n=1}^{\infty} \sum_{m=-n}^n \sum_{p=1 \neq p'}^2 {}^s C_{mnp}^l |mn3p\rangle, \quad (3)$$

because of the simple relation between the \mathbf{E} field and the \mathbf{H} field, and the relations between the normal modes: $\mathbf{H} = 1/i\omega\mu \nabla \times \mathbf{E}$, $\mathbf{N} = 1/k \nabla \times \mathbf{M}$, $\mathbf{M} = 1/k \nabla \times \mathbf{N}$.¹⁷ Hence, the computational problem is how to represent the function T in Eq. (2) in a more efficient way to facilitate calculations.

3. NUMERICAL METHODS

To calculate the scattering field for ensembles of nanospheres expediently, we define the following matrix:

where N is the number from which higher numbers of multipoles are truncated, M is the maximum angular number with $M \leq N$, c_n^l and d_n^l are the penetrating Lorenz–Mie coefficients, and the superscript D transfers the elements in the vector to the corresponding diagonal elements in the matrix with zero nondiagonal elements. The selection of M and N depends on the requirements of the convergence in the simulations. Based on the above matrix, we then construct the following matrix:

$$G_l = [X_1^l \quad X_2^l],$$

$${}^l W_1^E = [Y_{11}^l \quad Y_{12}^l]^T,$$

$${}^l W_1^H = [Y_{12}^l \quad Y_{11}^l]^T,$$

$${}^l W_3^E = [Y_{31}^l \quad Y_{32}^l]^T,$$

$${}^l W_3^H = [Y_{32}^l \quad Y_{31}^l]^T,$$

$$S_l = \begin{bmatrix} Z_1^l & 0 \\ 0 & Z_2^l \end{bmatrix},$$

$$X_p^l = [iC_{-11p}^l \quad iC_{01p}^l \quad iC_{11p}^l \quad iC_{-22p}^l \quad iC_{-12p}^l \quad iC_{021}^l \quad iC_{12p}^l \quad iC_{22p}^l \quad \dots \quad iC_{-MNp}^l \quad iC_{-(M-1)Np}^l \quad \dots \quad iC_{MNp}^l],$$

$$Y_{jp}^l = [|-11jp\rangle^l \quad |01jp\rangle^l \quad |11jp\rangle^l \quad |-22jp\rangle^l \quad \dots \quad |22jp\rangle^l \quad \dots \quad |-MNjp\rangle^l \quad \dots \quad |MNjp\rangle^l],$$

$$Z_1^l = [b_1^l \quad b_1^l \quad b_1^l \quad b_2^l \quad b_2^l \quad b_2^l \quad b_2^l \quad b_2^l \quad \dots \quad b_N^l \quad \dots \quad b_N^l]^D,$$

$$Z_2^l = [a_1^l \quad a_1^l \quad a_1^l \quad a_2^l \quad a_2^l \quad a_2^l \quad a_2^l \quad a_2^l \quad \dots \quad a_N^l \quad \dots \quad a_N^l]^D,$$

$$U_1^l = [d_1^l \quad d_1^l \quad d_1^l \quad d_2^l \quad d_2^l \quad d_2^l \quad d_2^l \quad d_2^l \quad \dots \quad d_N^l \quad \dots \quad d_N^l]^D,$$

$$U_2^l = [c_1^l \quad c_1^l \quad c_1^l \quad c_2^l \quad c_2^l \quad c_2^l \quad c_2^l \quad c_2^l \quad \dots \quad c_N^l \quad \dots \quad c_N^l]^D,$$

$${}^l h \bar{A} = \begin{bmatrix} {}^l h A_{-11}^{-11} & {}^l h A_{01}^{-11} & {}^l h A_{11}^{-11} & {}^l h A_{-22}^{-11} & \dots & {}^l h A_{22}^{-11} & \dots & {}^l h A_{-MN}^{-11} & \dots & {}^l h A_{MN}^{-11} \\ {}^l h A_{-11}^{01} & {}^l h A_{01}^{01} & {}^l h A_{11}^{01} & {}^l h A_{-22}^{01} & \dots & \cdot & \dots & \cdot & \dots & \cdot \\ {}^l h A_{-11}^{11} & {}^l h A_{01}^{11} & {}^l h A_{11}^{11} & {}^l h A_{-22}^{11} & \dots & \cdot & \dots & \cdot & \dots & \cdot \\ {}^l h A_{-11}^{-22} & {}^l h A_{01}^{-22} & {}^l h A_{11}^{-22} & {}^l h A_{-22}^{-22} & \dots & \cdot & \dots & {}^l h A_{-MN}^{-22} & \dots & {}^l h A_{MN}^{-22} \\ \vdots & \vdots & \vdots & \vdots & \ddots & \vdots & \ddots & \vdots & \ddots & \vdots \\ {}^l h A_{-11}^{22} & \cdot & \cdot & \cdot & \cdot & {}^l h A_{22}^{22} & \dots & \cdot & \dots & \cdot \\ \vdots & \vdots & \vdots & \vdots & \ddots & \vdots & \ddots & \vdots & \ddots & \vdots \\ {}^l h A_{-11}^{-MN} & \cdot & \cdot & {}^l h A_{-22}^{-MN} & \dots & \cdot & \dots & \cdot & \dots & \cdot \\ \vdots & \vdots & \vdots & \vdots & \ddots & \vdots & \ddots & \vdots & \ddots & \vdots \\ {}^l h A_{-11}^{MN} & \cdot & \cdot & {}^l h A_{-22}^{MN} & \dots & \cdot & \dots & \cdot & \dots & {}^l h A_{MN}^{MN} \end{bmatrix},$$

$${}^l h \bar{B} = \begin{bmatrix} {}^l h B_{-11}^{-11} & {}^l h B_{01}^{-11} & {}^l h B_{11}^{-11} & {}^l h B_{-22}^{-11} & \dots & {}^l h B_{22}^{-11} & \dots & {}^l h B_{-MN}^{-11} & \dots & {}^l h B_{MN}^{-11} \\ {}^l h B_{-11}^{01} & {}^l h B_{01}^{01} & {}^l h B_{11}^{01} & {}^l h B_{-22}^{01} & \dots & \cdot & \dots & \cdot & \dots & \cdot \\ {}^l h B_{-11}^{11} & {}^l h B_{01}^{11} & {}^l h B_{11}^{11} & {}^l h B_{-22}^{11} & \dots & \cdot & \dots & \cdot & \dots & \cdot \\ {}^l h B_{-11}^{-22} & {}^l h B_{01}^{-22} & {}^l h B_{11}^{-22} & {}^l h B_{-22}^{-22} & \dots & \cdot & \dots & {}^l h B_{-MN}^{-22} & \dots & {}^l h B_{MN}^{-22} \\ \vdots & \vdots & \vdots & \vdots & \ddots & \vdots & \ddots & \vdots & \ddots & \vdots \\ {}^l h B_{-11}^{22} & \cdot & \cdot & \cdot & \cdot & {}^l h B_{22}^{22} & \dots & \cdot & \dots & \cdot \\ \vdots & \vdots & \vdots & \vdots & \ddots & \vdots & \ddots & \vdots & \ddots & \vdots \\ {}^l h B_{-11}^{-MN} & \cdot & \cdot & {}^l h B_{-22}^{-MN} & \dots & \cdot & \dots & \cdot & \dots & \cdot \\ \vdots & \vdots & \vdots & \vdots & \ddots & \vdots & \ddots & \vdots & \ddots & \vdots \\ {}^l h B_{-11}^{MN} & \cdot & \cdot & {}^l h B_{-22}^{MN} & \dots & \cdot & \dots & \cdot & \dots & {}^l h B_{MN}^{MN} \end{bmatrix}, \quad (4)$$

$$P_l = \begin{bmatrix} U_1^l & 0 \\ 0 & U_2^l \end{bmatrix},$$

$$\Omega_{lh} = \begin{bmatrix} {}^{lh}\bar{A} & {}^{lh}\bar{B} \\ {}^{lh}\bar{B} & {}^{lh}\bar{A} \end{bmatrix}. \quad (5)$$

For a single particle, the scattering matrix and the scattered field are easily written as

$${}^1T = GS,$$

$$\mathbf{E}_s = {}^1TW_3^E,$$

$$\mathbf{H}_s = \frac{k}{i\omega\mu} {}^1TW_3^H. \quad (6)$$

For the ensemble of two spheres, we have to consider different orders of scattering from different scatterers, if we do not treat it as a full-boundary problem. The scattering matrix of one of the spheres, which represents the outgoing wave from this sphere, is a sum of the different orders of scattering originated from this sphere as a result of the optical response to the incident field and the scattered field from the other sphere:

$${}^2T_1 = ({}^1T_1 + {}^1T_2\Omega_{21}S_1) \sum_{i=0}^{N_{os}} (\Omega_{12}S_2\Omega_{21}S_1)^i,$$

$${}^2T_2 = ({}^1T_2 + {}^1T_1\Omega_{12}S_2) \sum_{i=0}^{N_{os}} (\Omega_{21}S_1\Omega_{12}S_2)^i, \quad (7)$$

where N_{os} is the number of the scattering order, from which the higher orders will be ignored. $\Omega_{21}S_1$ represents the field that is scattered by sphere 2 and then scattered by sphere 1.

A three-particle system can be considered as a two-particle system plus one additional sphere. The scattering matrix of this additional sphere is represented by

$${}^3T_3 = ({}^1T_3 + {}^2T_1\Omega_{13}S_3) \sum_{i=0}^{N_{os}} (\Omega_{31}S_1\Omega_{13}S_3)^i$$

$$+ ({}^1T_3 + {}^2T_2\Omega_{23}S_3) \sum_{i=0}^{N_{os}} (\Omega_{32}S_2\Omega_{23}S_3)^i - {}^1T_3. \quad (8)$$

It is easy to obtain the scattering matrix of one of the other two spheres by simply permuting the number of the subscripts:

$${}^3T_1 = ({}^1T_1 + {}^2T_3\Omega_{31}S_1) \sum_{i=0}^{N_{os}} (\Omega_{13}S_3\Omega_{31}S_1)^i$$

$$+ ({}^1T_1 + {}^2T_2\Omega_{21}S_1) \sum_{i=0}^{N_{os}} (\Omega_{12}S_1\Omega_{21}S_1)^i - {}^1T_1,$$

$${}^3T_2 = ({}^1T_2 + {}^2T_1\Omega_{12}S_2) \sum_{i=0}^{N_{os}} (\Omega_{21}S_1\Omega_{12}S_2)^i$$

$$+ ({}^1T_3 + {}^2T_3\Omega_{32}S_2) \sum_{i=0}^{N_{os}} (\Omega_{23}S_3\Omega_{32}S_2)^i - {}^1T_2. \quad (9)$$

In general, an L -particle system can be considered as an $(L-1)$ -particle system plus one additional sphere. The scattering matrix of this additional sphere is represented as

$${}^L T_L = \sum_{j=1}^{L-1} ({}^1T_L + {}^{L-1}T_j\Omega_{jL}S_L) \sum_{i=0}^{N_{os}} (\Omega_{Lj}S_j\Omega_{jL}S_L)^i$$

$$- (L-2) {}^1T_L. \quad (10)$$

The scattering matrix of any l th sphere can be obtained similarly to Eqs. (9) as

$${}^L T_l = \sum_{j=1 \neq l}^L ({}^1T_l + {}^{L-1}T_j\Omega_{jl}S_l) \sum_{i=0}^{N_{os}} (\Omega_{lj}S_j\Omega_{jl}S_l)^i$$

$$- (L-2) {}^1T_l. \quad (11)$$

The total scattered field is then written as

$$\mathbf{E}_s = \sum_{l=1}^{\oplus L} \mathbf{E}_s^l = \sum_{l=1}^{\oplus L} {}^L T_l {}^l W_3^E,$$

$$\mathbf{H}_s = \sum_{l=1}^{\oplus L} \mathbf{H}_s^l = \frac{k}{i\omega\mu} \sum_{l=1}^{\oplus L} {}^L T_l {}^l W_3^H. \quad (12)$$

It is not difficult to obtain the penetrating field inside any l th particle as

$$\mathbf{E}_p^l = \frac{{}^L T_l}{S_l} P_l {}^l W_1^E,$$

$$\mathbf{H}_p^l = \frac{k} {i\omega\mu} \frac{{}^L T_l}{S_l} P_l {}^l W_1^H. \quad (13)$$

Hence, we have a recursive solution to the scattering matrix of any number of spheres. It should be noted that the size of the scattering matrix is fixed when the maximum multipole number N and the maximum angular number M are chosen, whatever the numbers of spheres. Such a case can certainly facilitate calculations, since for the ordinary T-matrix method, the size of the scattering matrix will increase as L^2 . It is also worthwhile knowing that the scattering orders can be accounted for to the infinite order by the matrix inverse, i.e., $\sum_{i=0}^{\infty} (\Omega_{kj}S_j\Omega_{jk}S_k)^i = 1/(1 - \Omega_{kj}S_j\Omega_{jk}S_k)$ in principle. But the matrix inverse is usually not applicable for large scattering matrices because of either longer computational time or singularity problems.

4. NUMERICAL EXAMPLES

Figure 1 gives an example of calculations of the local field of three Ag spheres with different incident polarizations. It is clear that the local field intensity varies with the in-

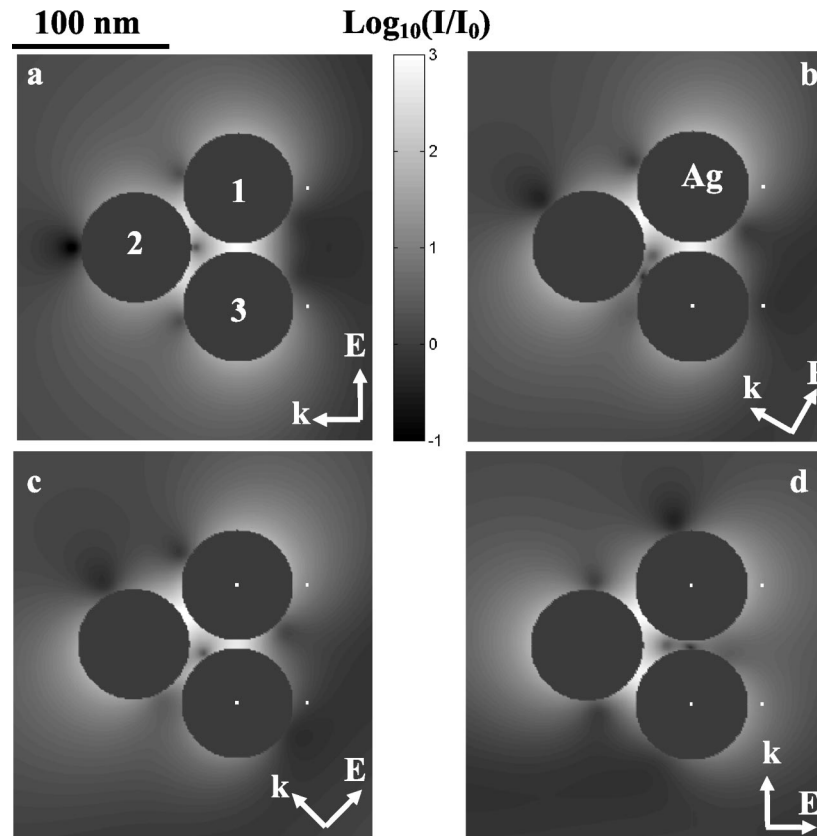


Fig. 1. Local intensity enhancement distribution I/I_0 in logarithmic scale in the plane of the wave vector \mathbf{k} and the electric field \mathbf{E} through the centers of three identified Ag spheres with radius $R = 35$ nm at the incident wavelength 514.5 nm for different incident polarizations as illustrated by the arrows of \mathbf{E} and \mathbf{k} . The dielectric function of Ag is obtained from Johansson and Christy.²¹ The number of the multipoles is $L = 16$ and the orders of scattering $N_{os} = 200$, which are enough for the convergence of the calculations.

cident polarization. For a two-particle system, such an effect has been demonstrated clearly by the recent experiment with surface-enhanced Raman scattering.²⁰ The surface-enhanced Raman scattering signals of the dimers reached maximum when the incident field was parallel to the axes of the dimers, while there was no enhancement at all when the incident field was perpendicular to the axes of the dimers. The experiment indicates that interparticle coupling is driven by the electric field that is aligned with the axis of the dimer. For the current case of the triplet, the interparticle coupling still seems driven by the component of the electrical field parallel to the axis of any two particles, but the local field intensity distribution is affected by the presence of the additional particle. For example, the local intensity in the cavity between sphere 1 and sphere 3 is strongly enhanced—more than 1000 times in Fig. 1a, where the incident electrical field is parallel to the axis of these two spheres. In the meantime, the local intensity in the cavity between sphere 1 and sphere 2, and the cavity between sphere 2 and sphere 3 is also enhanced, but not so much. When the incident field is perpendicular to the axis of two spheres, e.g., sphere 2 and sphere 3 in Fig. 1b, no enhancement can be found in the cavity between those spheres, but the couplings between sphere 1 and 3 and sphere 1 and 2 are still strong because of the component of the electrical field in the directions of the axes. In Fig. 1c, where the incident polarization was rotated slightly from that in Fig. 1b, the

local intensity in the cavity between sphere 2 and sphere 3 starts to increase.

Fig. 1d is quite similar to Fig. 1b, just by changing the incident polarization \mathbf{E} to be perpendicular to the axis of sphere 1 and 3 instead of the axis of sphere 2 and 3 in Fig. 1b. The purpose of showing this case is to demonstrate the validity of the calculations. Since the coordinates of the three particles are fixed in the different polarization calculations, the expansion coefficients of the incident field and the scattered field will be totally different if we vary the incident polarization \mathbf{E} and the incident wave vector \mathbf{k} . But the numerical results from the different processes are indeed the same when they are expected to be. The validation is confirmed by other, different, calculations also.

For systems with more spheres, the entangled coupling becomes more complex. Figure 2 shows an example of five Ag spheres with different sizes. The local field in the cavities between the particles is greatly enhanced, but the variation with incident polarization is not as significant as in Fig. 1. The reason is that the interparticle coupling caused by the scattered field from other neighboring spheres becomes stronger, hence they lose the incident polarization sensitivity.

5. SUMMARY

In summary, we have presented a recursive numerical method for solving the light scattering of ensembles of

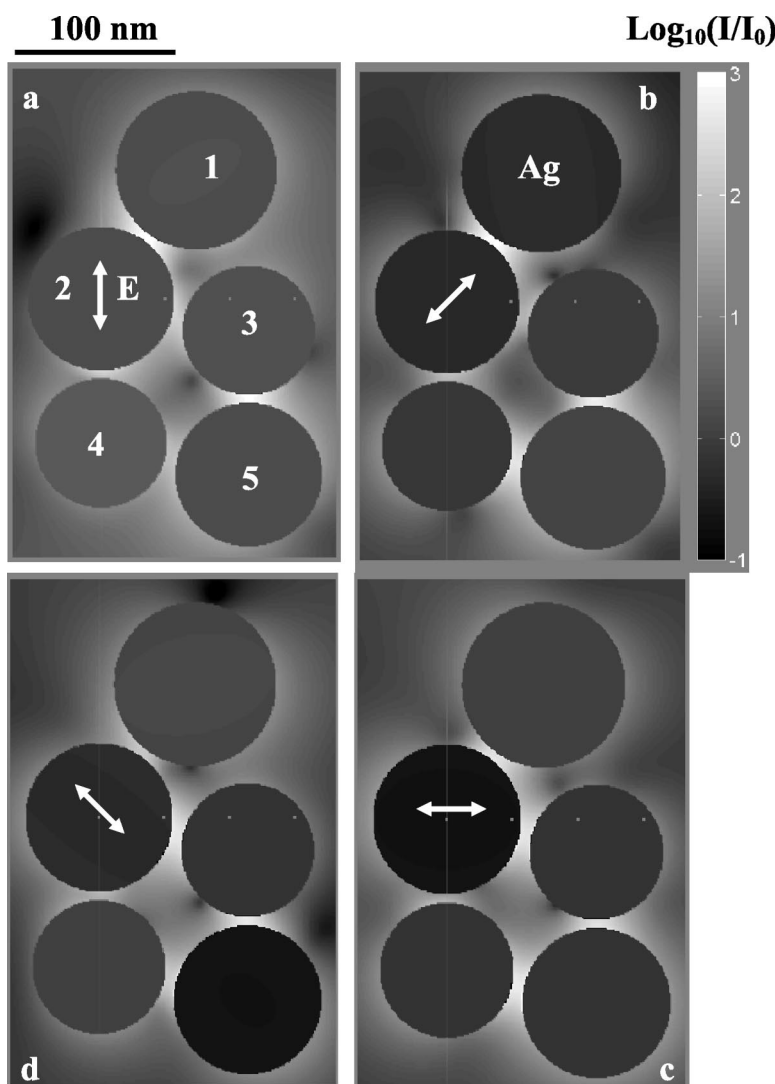


Fig. 2. Local intensity distribution I/I_0 in the logarithmic scale in the plane through the centers of five different Ag spheres; 1 ($R = 55$ nm), 2 ($R = 50$ nm), 3 ($R = 45$ nm), 4 ($R = 45$ nm), and 5 ($R = 50$ nm) at the incident wavelength 514.5 nm, with the wave vector \mathbf{k} perpendicular to this plane and the different incident polarization \mathbf{E} illustrated by the white arrows. The number of the multipoles is $L = 16$ and the orders of scattering $N_{os} = 200$.

any number of particles by extending Mie theory; this method makes it possible to calculate the optical near field concisely. The examples of calculations show the validity of the current method. As a result of the numerical possibilities, the current numerical method can easily be applied in many fields, e.g., surface-enhanced Raman scattering, apertureless scanning near-field optical microscopy, photonic crystals, and surface plasmon photonics.

ACKNOWLEDGMENTS

The author gratefully acknowledges financial support from the Nanometer Consortium, Lund University, Sweden, under the leadership of Lars Samuelson, the Swedish Foundation for Strategic Research, and the Swedish Natural Science Research Council.

H. Xu's e-mail address is hongxing.xu@ftf.lth.se.

REFERENCES

1. M. Ohtsu, *Near-Field Nano-Optics* (Kluwer/Plenum, New York, 2000).
2. R. Hillenbrand and F. Keilmann, "Complex optical constants on a subwavelength scale," *Phys. Rev. Lett.* **85**, 3029–3032 (2000).
3. J. Prikulis, H. X. Xu, L. Gunnarsson, and M. Käll, "Phase-sensitive near-field imaging of metal nanoparticles," *J. Appl. Phys.* **92**, 6211–6213 (2002).
4. For SERS reviews, see M. Moskovits, "Surface-enhanced spectroscopy," *Rev. Mod. Phys.* **57**, 783–826 (1985).
5. K. Kneipp, H. Kneipp, I. Itzkan, R. R. Dasari, and M. S. Feld, "Ultrasensitive chemical analysis by Raman spectroscopy," *Chem. Rev.* **99**, 2957–2975 (1999).
6. M. Moskovits, L. L. Tay, J. Yang, and T. Haslett, "SERS and the single molecule," *Top. Appl. Phys.* **82**, 215–226 (2002).
7. L. Novotny, R. X. Bian, and X. S. Xie, "Theory of nanometric optical tweezers," *Phys. Rev. Lett.* **79**, 645–648 (1997).
8. H. X. Xu and M. Käll, "Surface-plasmon-enhanced optical forces in silver nanoaggregates," *Phys. Rev. Lett.* **89**, 246802 (2002).
9. X. H. Wang, R. Z. Wang, B. Y. Gu, and G. Z. Yang, "Decay

- distribution of spontaneous emission from an assembly of atoms in photonic crystals with pseudogaps," *Phys. Rev. Lett.* **88**, 093902 (2002).
10. U. Kreibig and M. Vollmer, *Optical Properties of Metal Clusters* (Springer, New York, 1995), pp. 155–173.
 11. G. Mie, "Beitrage zur optik truber medien speziell kolloidaler metallösungen," *Ann. Phys. (Leipzig)* **25**, 377–445 (1908).
 12. J. H. Bruning and Y. T. Lo, "Multiple scattering of EM waves by spheres. 1. Multipole expansion and ray-optical solution," *IEEE Trans. Antennas Propag.* **AP-19**, 378–390 (1971).
 13. Y. L. Xu, "Electromagnetic scattering by an aggregate of spheres," *Appl. Opt.* **34**, 4573–4588 (1995).
 14. D. W. Mackowski and M. I. Mishchenko, "Calculation of total cross sections of multiple-sphere clusters," *J. Opt. Soc. Am. A* **13**, 2266–2278 (1996).
 15. K. A. Fuller, "Optical resonances and 2-sphere system," *Appl. Opt.* **30**, 4716–4731 (1991).
 16. H. X. Xu, "A new method by extending Mie theory to calculate local field in outside/inside of aggregates of arbitrary spheres," *Phys. Lett. A* **312**, 411–419 (2003).
 17. J. A. Stratton, *Electromagnetic Theory* (McGraw-Hill, New York, 1941).
 18. S. Stein, "Addition theorems for spherical wave functions," *Q. Appl. Math.* **19**, 15–24 (1961).
 19. O. R. Cruzan, "Translational additional theorems for spherical vector wave functions," *Q. Appl. Math.* **20**, 33–40 (1962).
 20. H. X. Xu and M. Käll, "Polarization dependent surface-enhanced Raman spectroscopy of isolated silver nanoaggregates," *ChemPhysChem* **4**, 1001–1005 (2003).
 21. P. B. Johanson and R. W. Christy, "Optical constants of noble metals," *Phys. Rev. B* **6**, 4370–4379 (1972).